SUPPLEMENTARY INFORMATION

Oligonucleotides

Fluorescence polarization and sedimentation velocity:

40bot-FITC (5′-FAM-gtgttcggactctgcctcaagacggtagtcaacgtgcttg)

and complementary oligonucleotide:

40top (5′-caagcacgttgactaccgtcttgaggcagagtccgaacac),

In SAXS experiments oligonucleotides without fluorescent label were used.

Exonuclease, ATPase and nucleotide binding:

Three base-loop hairpin oligonucleotide (22 bp double stranded region),

Exo-flash: (5’ ctccgcccgcagcgcgcccgcc tgt ggcgggcgcgctgcgggcgg[2AmPur]g)

Endonuclease assay:

Three base-loop hairpin oligonucleotides (22 bp double stranded region),

L3-flash: (5’ ctccgcccgcagcgcgcccgcc tgt ggcgggcgcgctgcgggcggag),

L3-5A:(5’aaaaaactccgcccgcagcgcgcccgcc tgt ggcgggcgcgctgcgggcggag),

L3-3A: (5’ ctccgcccgcagcgcgcccgcc tgt ggcgggcgcgctgcgggcggagaaaaaa),

L3-3,5A: (5’ aaaaaactccgcccgcagcgcgcccgcc tgt ggcgggcgcgctgcgggcggagaaaaaa)

Nine base-loop hairpin oligonucleotides (22 bp double stranded region),

L9-flash: (5’ ctccgcccgcagcgcgcccgcc ctttgtttc ggcgggcgcgctgcgggcggag),

L9-5A:(5’aaaaaactccgcccgcagcgcgcccgcc ctttgtttc ggcgggcgcgctgcgggcggag),

L9-3A: (5’ ctccgcccgcagcgcgcccgcc ctttgtttc ggcgggcgcgctgcgggcggagaaaaaa),

SUPPLEMENTAL FIGURE LEGENDS.

Figure S1. Nucleotide binding by RAD50 protein is in exchange with solution nucleotides

(A) Displacement kinetics of pre-bound ADP-TR from hMSH2/3 (left) or RAD50-L1 (right) with unlabeled ADP. The MSH2/3 and RAD50-L1 proteins (3 μM) were incubated with ADP-TR (5 nM) for 10 min. Displacement was initiated with the addition of 1 mM unlabelled ADP and the reaction was monitored as a decrease of the anisotropy signal using excitation and emission wavelength of 595 and 615 nm respectively. Experimental displacement data (red); the fit to single exponential decay model (blue). **(B)** Resolution of crosslinked products by SDS-PAGE. Reactions contained 1 mM [α-^{32}P]-ATP and 30 μM of the indicated protein. UV Crosslinking of labeled nucleotides to the complexes was performed in a Stratalinker 1800 (Stratagene) for 7.5 minutes and the products were resolved by SDS-PAGE. Two different exposures are shown for lanes (1) hMSH2/3, (2) L1, (3) L4, (4) L1-MRE11, (5) L4-MRE11, (6) MRE11-RAD50 FL.

Figure S2. AMP-PNP binds to L4-MRE11 with low affinity.

ATP (red), AMP-PNP (dark blue), ATP-γS (dark green), ADP (light blue) and ADP-BeF_n (light-green) were added as competitors at the indicated concentrations for L4-MRE11 (1 μM) pre-bound with ATP-ATTO 488 (2 μM binding sites). Anisotropy was measured with a TECAN plate reader using excitation and emission wavelengths of 470 and 522 nm respectively. The K_i values were calculated using a competitive binding mass action model.

Figure S3. FRET analysis of nucleotides binding to L1, L4, L1-MRE11 and L4-MRE11 proteins.

(A) Normalized FRET was calculated as the ratio of energy transfer to the intensity of the donor, and normalized for the signal arising from the reaction containing no protein (as described in the

legend to the Figure 2). Symbols are as described in Figure 2B,C The schematic diagram of the "closed" complexes derived from the FRET results for L4 **(B)** and L4-MRE11 **(C)** after ATP binding.

Figure S4. Endonuclease Assays with L9 DNA substrates.

(A) Schematic representations of the DNA hairpin substrates for each gel panel. The asterisk marks the position of the ^{32}P label. **(B)** Each assay contained 0.5 μM protein, 0.5 μM DNA, 1 mM ATP (where indicated), and either 5 mM $MnCl_2$ alone or both 5 mM $MgCl_2$ and 1 mM $MnCl_2$. Aliquots were quenched at 0 minutes and 60 minutes and the products were resolved on SDS-PAGE gels. (+) and (-) indicate the presence or absence of nucleotide. **(C)** Endonuclease activity is observed for the L9/5'A and L9/3'A substrates in the presence of ATP. The new band visible in the L9/3'A samples migrates with the same mobility as the L9 substrate without an overhang, indicating that the overhang was removed.

Figure S5. Exo –endonuclease switch and staggered DNA ends.

Possible uses of the ATP driven switch between RAD50 endo- and exonuclease activity in 'cleaning' the staggered ends (left) or in removing protein adducts (right).

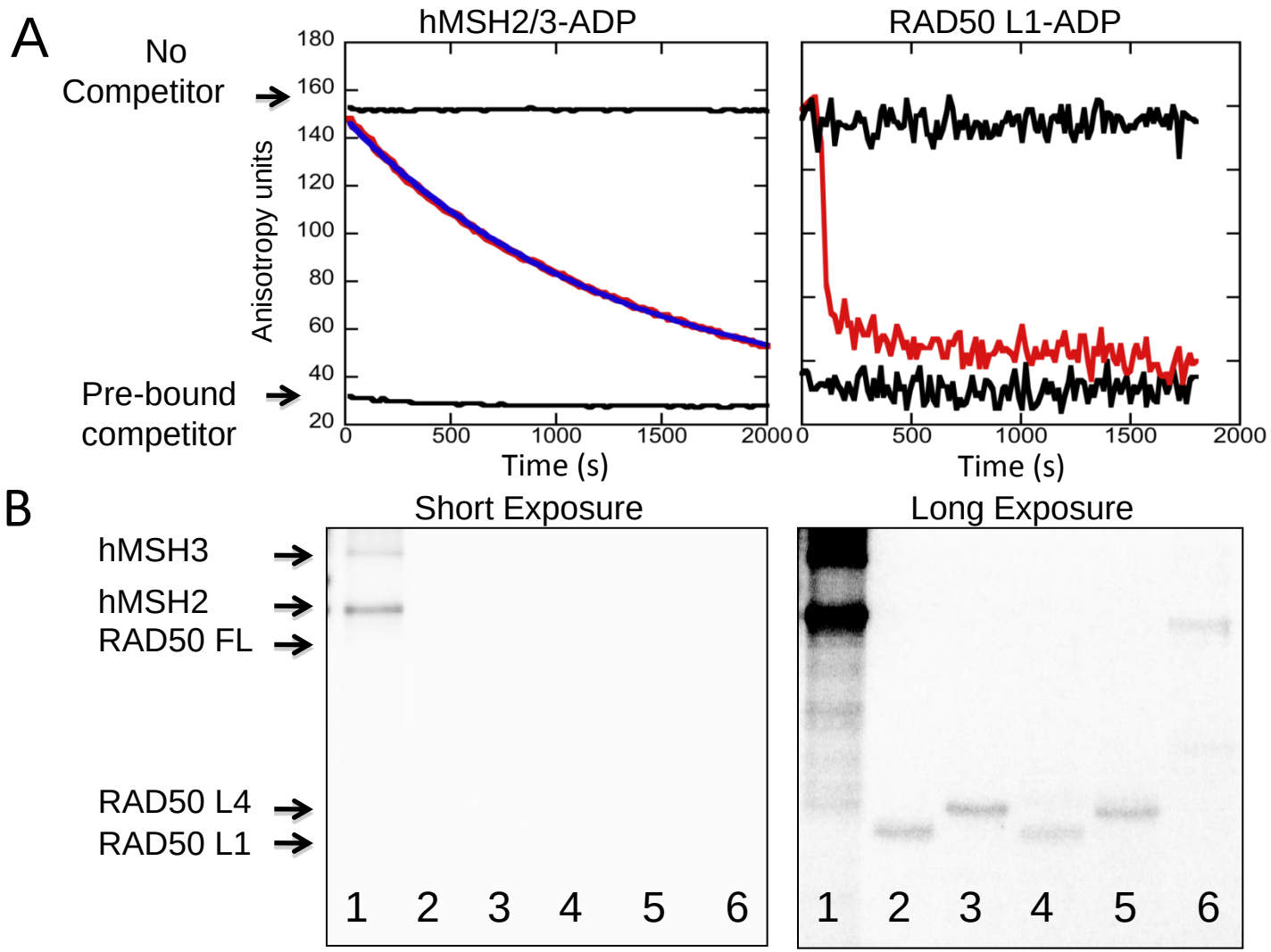

Figure S1. Nucleotide binding by RAD50 protein is in exchange with solution nucleotides
(A) Displacement kinetics of pre-bound ADP-TR from hMSH2/3 (left) or RAD50-L1 (right) with unlabeled ADP. The MSH2/3 and RAD50-L1 proteins (3 μM) were incubated with ADP-TR (5 nM) for 10 min. Displacement was initiated with the addition of 1 mM unlabelled ADP and the reaction was monitored as a decrease of the anisotropy signal using excitation and emission wavelength of 595 and 615 nm respectively. Experimental displacement data (red); the fit to single exponential decay model (blue). **(B)** Resolution of crosslinked products by SDS-PAGE. Reactions contained 1 mM [α-^{32}P]-ATP and 30 μM of the indicated protein. UV Crosslinking of labeled nucleotides to the complexes was performed in a Stratalinker 1800 (Stratagene) for 7.5 minutes and the products were resolved by SDS-PAGE. Two different exposures are shown for lanes (1) hMSH2/3, (2) L1, (3) L4, (4) L1-MRE11, (5) L4-MRE11, (6) MRE11-RAD50 FL.

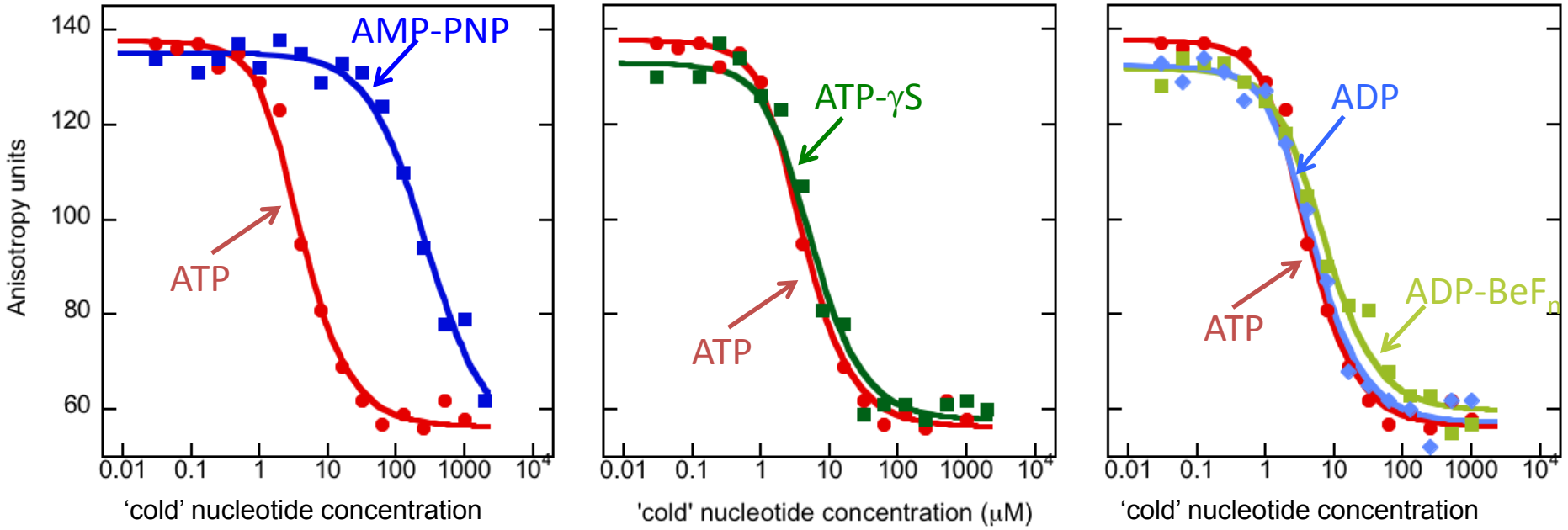

	K_I, (μM)
ATP	0.586 ± 0.082
AMP-PNP	60.8 ± 16
ATP-γS	0.899 ± 0.23
ADP-BeFn	0.944 ± 0.20
ADP	0.474 ± 0.071

Figure S2. AMP-PNP binds to L4-MRE11 with low affinity.
ATP (red), AMP-PNP (dark blu)e, ATP-γS (dark green), ADP light blue) and ADP-BeF_n (light green) were added as competitors at the indicated concentrations to L4-MRE11(1μM) to pre-bound with with ATP-ATTO 488 (2μM binding sites). Anisotropy was measured with a TECAN plate reader using excitation and emission wavelength of 470 and 522 nm respectively. The K_I values (Table 1) were calculated using competitive binding mass action model.

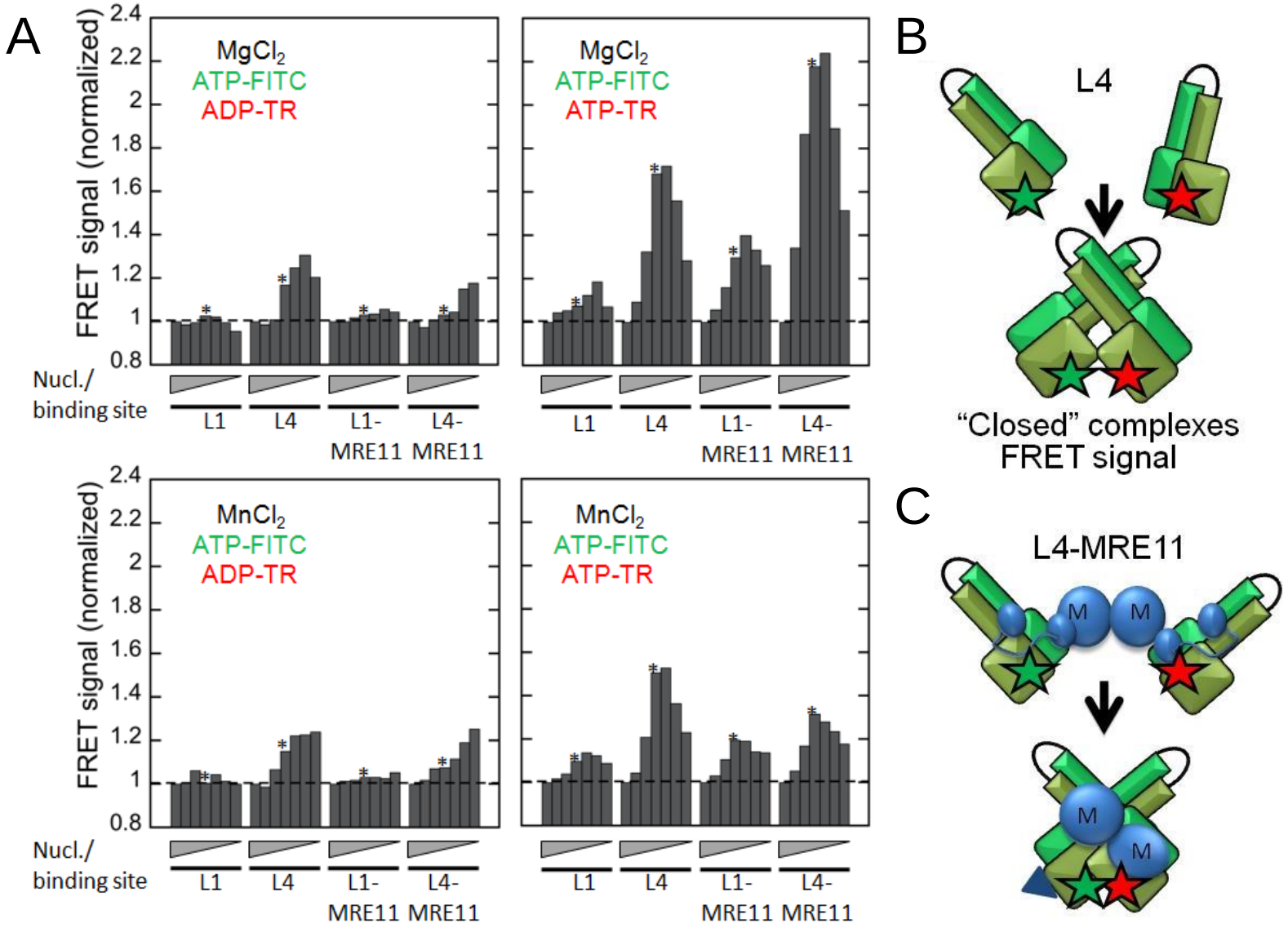

Figure S3. FRET analysis of nucleotides binding to L1, L4, L1-MRE11 and L4-MRE11 proteins.
(A) Normalized FRET was calculated as the ratio of energy transfer to the intensity of the donor, and normalized for the signal arising for the reaction containing no protein (as described in the legend to the figure 2). Symbols are as described in Figure 2B,C The schematic diagram of the "closed" complexes derived from the FRET results for L4 **(B)** and L4-MRE11 **(C)** after ATP binding.

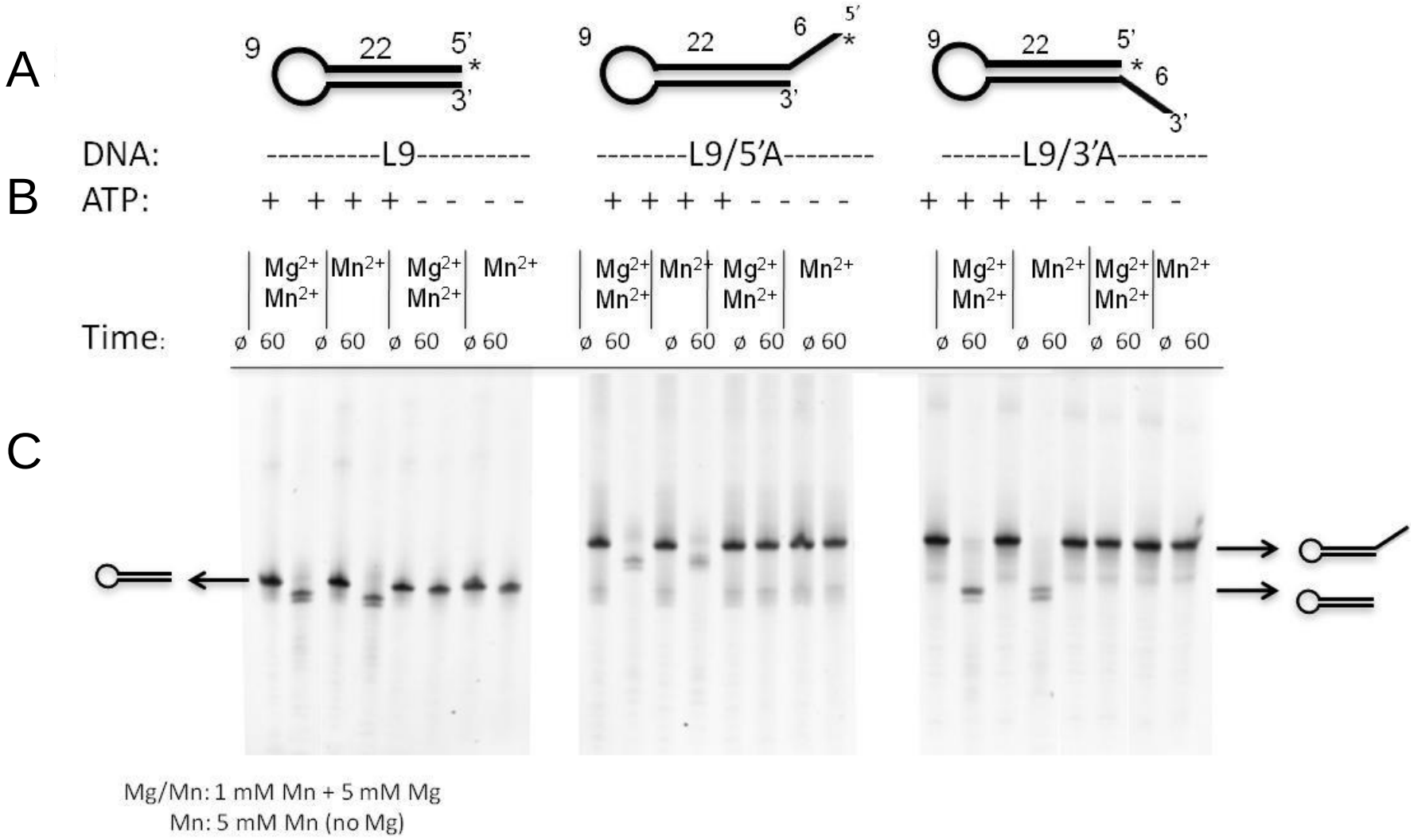

Figure S4. Endonuclease Assays with L9 DNA substrates.
(A) Schematic representations of the DNA hairpin substrates for each gel panel. The asterisk marks the position of the ^{32}P label. **(B)** Each assay contained 0.5 mM protein, 0.5 mM DNA, 1 mM ATP (where indicated), and either 5 mM $MnCl_2$ alone or both 5 mM $MgCl_2$ and 1 mM $MnCl_2$. Aliquots were quenched at 0 minutes and 60 minutes and the products were resolved on SDS-PAGE gels. (+) and (-) indicate the presence or absence of nucleotide. **(C)** Endonuclease activity is observed for the L9/5'A and L9/3'A substrates in the presence of ATP. The new band visible in the L9/3'A samples migrates with the same mobility as the L9 substrate without an overhang, indicating that the overhang was removed.

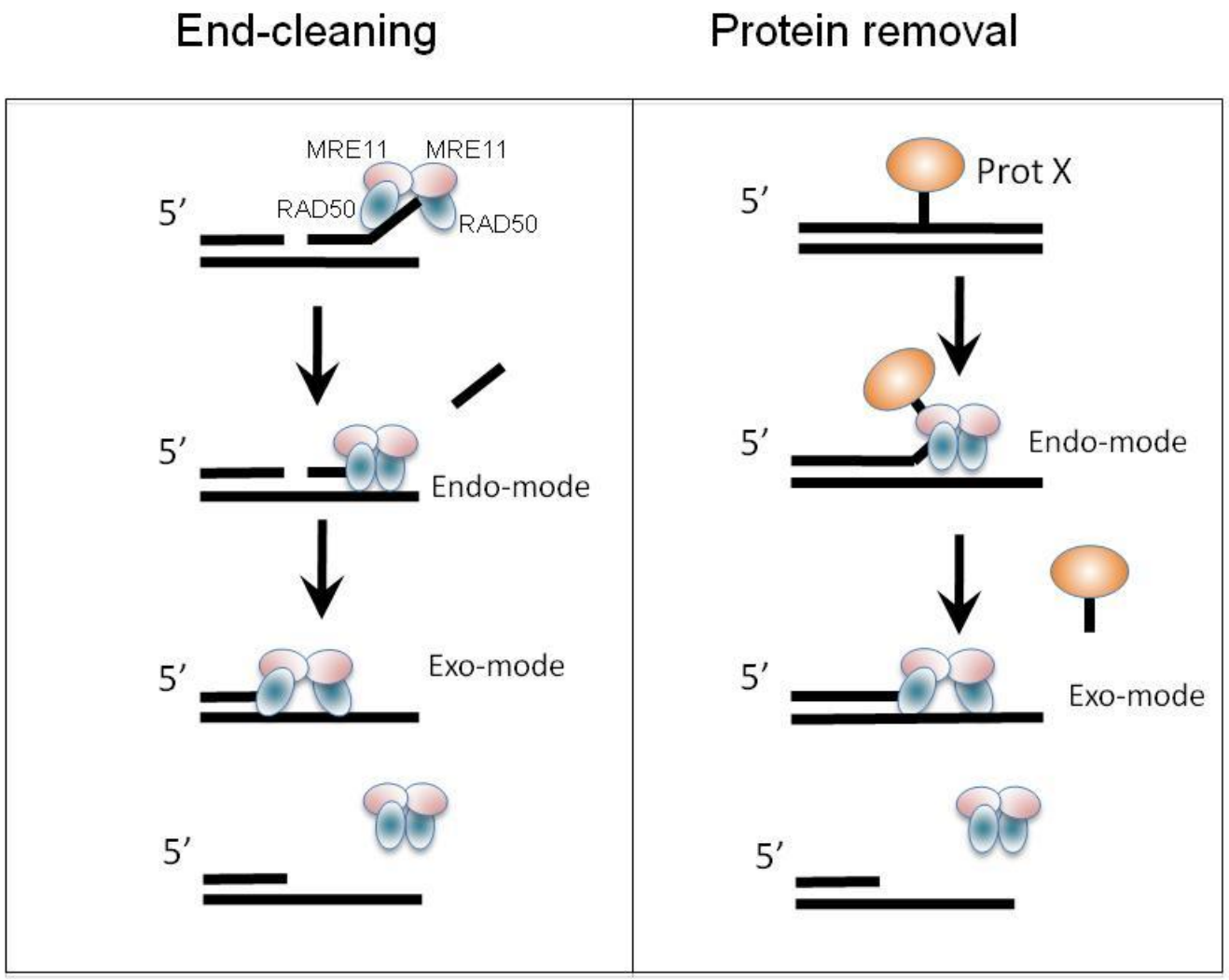

Figure S5. Exo –endonuclease switch and staggered DNA ends.
Possible uses of the ATP driven switch between RAD50 endo- and exonulease activity in ‘cleaning’ the staggered ends (left) or in removing protein adducts (right)

Table SI. The influenxe of DNA on nucleotide binding

	RAD50 L4		RAD50 L4/MRE11	
	$K_{D,\ ATP}$ (μM)	$K_{D,\ ADP}$ (μM)	$K_{D,\ ATP}$ (μM)	$K_{D,\ ADP}$ (μM)
Mg^{2+}	1.94 ± 0.10	0.254 ± 0.043	1.05 ± 0.12	0.260 ± 0.051
DNA-Mg^{2+}	3.50 ± 0.31	0.663 ± 0.15	1.59 ± 0.20	0.504 ± 0.10
Mn^{2+}	2.46 ± 0.18	0.646 ± 0.19	0.853 ± 0.063	0.280 ± 0.069
DNA-Mn^{2+}	2.72 ± 0.62	1.10 ± 0.25	1.27 ± 0.21	0.423 ± 0.12

Table SII. RAD50-MRE11 affinity for DNA (K_d in μM)

$MRE11_{1-342}$						
	SS DNA			**DS DNA**		
	-	Mg^{2+}	Mn^{2+}	-	Mg^{2+}	Mn^{2+}
No ATP	0.41 ± 0.06	0.73 ± 0.011	0.034 ± 0.011	ND	ND	0.15 ± 0.04
ATP	0.61 ± 0.06	0.73 ± 0.08	0.035 ± 0.012	ND	ND	0.16 ± 0.04

L4						
	SS DNA			**DS DNA**		
	-	**Mg^{2+}**	**Mn^{2+}**	**-**	**Mg^{2+}**	**Mn^{2+}**
No ATP	0.33 ± 0.04	1.3 ± 0.2	0.82 ± 0.09	0.45 ± 0.05	1.8 ± 0.4	1.1 ± 0.2
ATP	0.25 ± 0.03	0.62 ± 0.1	0.70 ± 0.04	0.37 ± 0.04	0.95 ± 0.1	1.5 ± 0.5

L4-MRE11								
	SS DNA				**DS DNA**			
	-	**Mg^{2+}**	**Mn^{2+}**	**Mg^{2+},Mn^{2+}**	**-**	**Mg^{2+}**	**Mn^{2+}**	**Mg^{2+},Mn^{2+}**
No ATP	0.72 ± 0.08	0.53 ± 0.05	0.034 ± 0.004	0.092 ± 0.01	0.71 ± 0.02	2.1 ± 0.9	0.18 ± 0.04	0.17 ± 0.04
ATP	1.2 ± 0.1	1.6 ± 0.2	0.098 ± 0.009	0.31 ± 0.06	1.1 ± 0.3	1.6 ± 0.5	0.4 ± 0.08	0.4 ± 0.06
ADP	0.89 ± 0.08	1.2 ± 0.1	0.057 ± 0.006	0.13 ± 0.03	1.7 ± 0.6	2.1 ± 1	0.4 ± 0.09	0.3 ± 0.1

Table SIII. Rates of MRE11 exonuclease activity

	MRE11(1-342)			L4-MRE11		
	K_M (μM)	**k_{cat} (min^{-1})**	**k_{cat}/K_M (min^{-1} μM^{-1})**	**K_M (μM)**	**k_{cat} (min^{-1})**	**k_{cat}/K_M (min^{-1} μM^{-1})**
Mn^{+2}						
No nucl.	4.1 ± 0.5	0.061 ± 0.002	**14.9 ± 1.9**	3.2 ± 0.4	0.026 ± 0.001	**8.1 ± 1.1**
ATP	2.7 ± 0.6	0.047 ± 0.003	**17.4 ± 4.02**	7.8 ± 0.6	0.046 ± 0.001	**5.9 ± 0.47**
ATPγS	1.9 ± 0.3	0.043 ± 0.002	**22.6 ± 3.73**	8.1 ± 1.3	0.040 ± 0.003	**4.9 ± 0.87**
ADP	9 ± 0.2	0.055 ± 0.001	**6.11 ± 0.18**	5.9 ± 0.7	0.037 ± 0.002	**6.3 ± 0.82**
Mn^{+2}, Mg^{+2}						
no nucl.	6.3 ± 1.9	0.093 ± 0.01	**14.8 ± 4.5**	10.3 ± 1.4	0.047 ± 0.003	**4.7 ± 0.70**
ATP	5.8 ± 0.9	0.088 ± 0.005	**15.2 ± 2.5**	21.2 ± 2.2	0.068 ± 0.004	**3.2 ± 0.38**
ATPγS	5.4 ± 0.8	0.088 ± 0.004	**16.3 ± 2.5**	6.7 ± 0.6	0.013 ± 0.001	**1.9 ± 0.23**
ADP	8.1 ± 0.2	0.114 ± 0.008	**14.1 ± 1.0**	16.6 ± 2.1	0.072 ± 0.004	**4.3 ± 0.60**